Broadband astigmatism-corrected Czerny–Turner spectrometer

Kye-Sung Lee,[1,*] Kevin P. Thompson,[2] and Jannick P. Rolland[1]

[1]*The Institute of Optics, University of Rochester, 275 Hutchinson Road, Rochester, New York 14627-0186, USA*
[2]*Optical Research Associates, 3 Graywood Lane, Pittsford, New York 14534, USA*
**kyelee@optics.rochester.edu*

Abstract: We report an optical design for a low-cost optics, broadband, astigmatism-corrected practical spectrometer. An off-the-shelf cylindrical lens is used to remove astigmatism over the full bandwidth. Results show that better than 0.1 nm spectral resolution and more than 50% throughput were achieved over a bandwidth of 400 nm centered at 800 nm.

OCIS codes: (120.6200) Spectrometers and spectroscopic instrumentation; (120.4570) Optical design of instruments; (110.4500) Optical coherence tomography.

References and links

1. A. F. Fercher, C. K. Hitzenberger, G. Kamp, and S. Y. El-Zaiat, "Measurement of intraocular distances by backscattering spectral interferometry," Opt. Commun. **117**(1-2), 43–48 (1995).
2. J. P. Rolland, P. Meemon, S. Murali, K. P. Thompson, and K. S. Lee, "Gabor-based fusion technique for Optical Coherence Microscopy," Opt. Express **18**(4), 3632–3642 (2010).
3. S. Murali, P. Meemon, K. S. Lee, W. P. Kuhn, K. P. Thompson, and J. P. Rolland, "Assessment of a liquid lens enabled in vivo optical coherence microscope," Appl. Opt. **49**(16), D145–D156 (2010).
4. A. S. Wyatt, I. A. Walmsley, G. Stibenz, and G. Steinmeyer, "Sub-10 fs pulse characterization using spatially encoded arrangement for spectral phase interferometry for direct electric field reconstruction," Opt. Lett. **31**(12), 1914–1916 (2006).
5. M. Czerny, and A. F. Turner, "On the Astigmatism of Mirror Spectrometers," Z. Phys. **61**(11-12), 792–797 (1930).
6. A. B. Shafer, L. R. Megill, and L. Droppleman, "Optimization of the Czerny-Turner spectrometer," J. Opt. Soc. Am. **54**(7), 879–887 (1964).
7. Q. Xue, S. Wang, and F. Lu, "Aberration-corrected Czerny-Turner imaging spectrometer with a wide spectral region," Appl. Opt. **48**(1), 11–16 (2009).
8. G. R. Rosendahl, "Contributions to the optics of mirror systems and gratings with oblique incidence. III. Some applications," J. Opt. Soc. Am. **52**(4), 412–415 (1962).
9. M. Goto and S. Morita, "Spatial distribution measurement of atomic radiation with an astigmatism-corrected Czerny–Turner-type spectrometer in the Large Helical Device," Rev. Sci. Instrum. **77**, 10F124 (2006).
10. A. B. Shafer, "Correcting for astigmatism in the czerny-turner spectrometer and spectrograph," Appl. Opt. **6**(1), 159–160 (1967).
11. M. L. Dalton, Jr., "Astigmatism compensation in the Czerny-turner spectrometer," Appl. Opt. **5**(7), 1121–1123 (1966).
12. B. Bates, M. McDowell, and A. C. Newton, "Correction of astigmatism in a Czerny–Turner spectrograph using a plane grating in divergent illumination," J. Phys. E **3**(3), 206–210 (1970).
13. M. McDowell, "Design of Czerny–Turner spectrographs using divergent grating illumination," Opt. Acta (Lond.) **22**, 473–475 (1975).
14. D. R. Austin, T. Witting, and I. A. Walmsley, "Broadband astigmatism-free Czerny-Turner imaging spectrometer using spherical mirrors," Appl. Opt. **48**(19), 3846–3853 (2009).
15. M. Born, and E. Wolf, *Principles of Optics*, (Cambridge University Press, 2002), Chap. 8.6.

1. Introduction

Two-beam spectral interferometry (SI) has enabled the rapid development of such techniques as spectrometer-based frequency-domain optical coherence tomography (FD-OCT) [1–3] and femtosecond pulse characterization [4]. The Czerny-Turner spectrometer is a commonly used instrument in SI because by definition, only two spherical mirrors and a plane grating can be configured in a coma-free geometry where, together with a low numerical aperture, spherical aberration can be avoided [5]. However, this solution simply does not provide resolution

#132486 - $15.00 USD Received 29 Jul 2010; revised 3 Oct 2010; accepted 4 Oct 2010; published 21 Oct 2010

better than 0.1 nm. The spectral resolution 0.1 nm is necessary for the application of FD-OCT to get 1 mm imaging depth in skin with submicron axial resolution, which is state-of-the-art in OCT. Czerny and Turner first showed that the coma aberration introduced by the off-axis reflection from a spherical mirror can be corrected by a symmetrical, but oppositely oriented, spherical mirror for spectrometer design [5]. After that, Shafer showed that the coma aberration can be still corrected in the Czerny-Turner spectrometer, even though its symmetry is broken, if the geometry parameters satisfy a condition that is known as the Shafer equation [6,7]. However, astigmatism remains in both configurations yielding different focal lengths in the tangential and sagittal planes. The astigmatism can be ignored in 1D spectroscopy by locating an exit slit at the tangential focal plane. However, some applications sensitive to power efficiency such as high speed spectrometer-based FD-OCT are required to collect most power with high speed line CCD or CMOS cameras where the width of the detector area is limited to maximize signal to noise ratio. In those applications, the uncorrected astigmatism does result in degraded performance. Some methods to reduce or remove the limiting astigmatism have been investigated such as, using additional convex mirrors [8], placing compensating optics before the entrance slit [9], using toroidal mirrors [6,10], using a cylindrical grating [11], or introducing divergent illumination [12–14]. Some techniques were pursued with a goal of providing extended spectral range. However, these methods need to satisfy a condition of the parameters of the Czerny-Turner spectrometer to compensate the astigmatism of the spectrometer [7,14], which may limit the spectrometer design for various specifications. Here we propose a novel solution also based on a modified Czerny-Turner geometry using only off-the-shelf, low-cost optical components without requiring the restrictive condition. Specifically, the solution includes all-spherical mirrors together with a cylindrical lens to compensate the astigmatism over a broadband width. This method enables low cost construction using off-shelf optics in place of components such a toroidal mirror or a cylindrical grating, both more complex elements to fabricate. We present how the cylindrical lens can remove the astigmatism over a broadband width and then show the design of the broadband astigmatism-corrected Czerny-Turner spectrometer and its result.

2. Broadband astigmatism compensation using a cylindrical lens

The difference in astigmatic foci generated by the two off-axis spherical mirrors of a Czerny-Turner can be written as [11]

$$\Delta_z = (R_1/2)\cdot(\sin\alpha_1 \tan\alpha_1) + (R_2/2)\cdot(\sin\alpha_2 \tan\alpha_2)\ , \qquad (1)$$

where R_1 is the radius of the first spherical mirror, R_2 is the radius of the second spherical mirror, α_1 is the off-axis incident angle on the first mirror, and α_2 is the off-axis incident angle on the second mirror. In our preferred design, a cylindrical lens is located near the detector as shown in Fig. 1 that displays both in (a) the tangential view and in (b) the sagittal view. The change of the sagittal focus $s_{cs} - s'_{cs}$ illustrated in Fig. 1(b) is calculated by the sagittal lens equation of the cylindrical lens $s'_{cs}{}^{-1}$ equal $f_{cs}{}^{-1} + s_{cs}{}^{-1}$, which yields

$$s_{cs} - s'_{cs} = s_{cs} - \left[f_{cs} s_{cs} / (f_{cs} + s_{cs}) \right]\ , \qquad (2)$$

where the subscript c stands for cylindrical, s_{cs} is the sagittal object distance, s'_{cs} is the sagittal image distance, and f_{cs} is the sagittal focal length of the cylindrical lens. The change of the tangential focus introduced by the cylindrical lens (i.e. plane parallel plates in the tangential view) is given simply by

$$s'_{ct} - s_{ct} = \left[(n-1)/n \right] \cdot t_0\ , \qquad (3)$$

where n is the refractive index and t_0 is the central thickness of the cylindrical lens.

The astigmatism is removed when

#132486 - $15.00 USD Received 29 Jul 2010; revised 3 Oct 2010; accepted 4 Oct 2010; published 21 Oct 2010

$$\Delta_z = s_{cs} - s'_{cs} + s'_{ct} - s_{ct} \ , \tag{4}$$

as illustrated in Fig. 1. Substituting the Eq. (2) and Eq. (3) into Eq. (4) gives

$$s_{cs}^2 - \left[\Delta_z - \left((n-1)/n\right)\, t_0\right] \cdot s_{cs} - f_{cs}\left[\Delta_z - \left((n-1)/n\right)\, t_0\right] = 0, \qquad s_{cs}\ \&\ f_{cs} > 0. \tag{5}$$

Solving for s_{cs} yields

$$s_{cs} = \left[P + \sqrt{P^2 + 4Pf_{cs}}\right] / 2 \ , \tag{6}$$

where $P = \Delta_z - t_0 \left(n-1\right)/n$. The position of the cylindrical lens is then determined as the distance from the second mirror L_c as shown in Fig. 1(b) given by

$$L_c = f_s - s_{cs} - t_0 \ , \tag{7}$$

where $f_s = R_2 / 2\cos\alpha_2$.

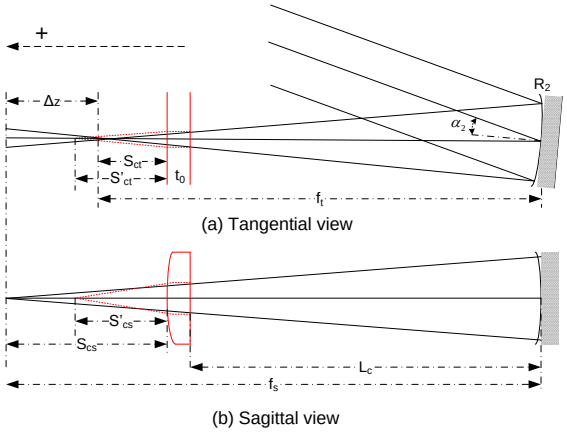

Fig. 1. Astigmatism correction by a cylindrical lens in (a) tangential view (b) sagittal view after the second mirror in a Czerny-Turner spectrometer.

The off-axis angle α_2 incident to the second spherical mirror varies according to the diffracted wavelength from the grating as shown in Fig. 2. The variation in α_2 across the second mirror results in a variation in astigmatism Δ_z across the detector. The Δ_z ascends ($R_2 > L_{GF}$, where L_{GF} is the distance between the grating and the second mirror) or descends ($R_2 < L_{GF}$) when the second mirror is rotated counter clockwise by $\bar{\alpha}_2$ from the perpendicular position at the central wavelength $\bar{\lambda}$. The ascending or descending astigmatism can be overall compensated by tilting of the cylindrical lens with an optimized angle. The differentiation $ds_{cs}/d\Delta$ is calculated from Eq. (6) as

$$ds_{cs} / d\Delta_z = \left(1/2\right) + \left[\left(P + 2f_{cs}\right) / \left(2\sqrt{P^2 + 4Pf_{cs}}\right)\right] . \tag{8}$$

The tilt angle ξ of the cylindrical lens with respect to the sagittal focal plane is shown in Fig. 2 and can be estimated with the first order polynomial fitting at the center (i.e. $H = 0$) as

$$\tan\xi \equiv \left(ds_{cs} / dH\right)\Big|_{H=0} = \left(ds_{cs} / d\Delta_z\right)\Big|_{\Delta_z=\bar{\Delta}_z} \cdot \left(d\Delta_z / d\lambda\right)\Big|_{\lambda=\bar{\lambda}} \cdot \left(d\lambda / dH\right)\Big|_{H=0} \ , \tag{9}$$

where $ds_{cs} / d\Delta_z\big|_{\Delta_z=\bar{\Delta}_z}$ is obtained from Eq. (8) as

#132486 - $15.00 USD Received 29 Jul 2010; revised 3 Oct 2010; accepted 4 Oct 2010; published 21 Oct 2010

$$\left(ds_{cs}/d\Delta_z\right)\Big|_{\Delta_z=\bar{\Delta}_z} = (1/2)+\left[\left(\bar{P}+2f_{cs}\right)/\left(2\sqrt{\bar{P}^2+4\bar{P}f_{cs}}\right)\right], \tag{10}$$

where $\bar{P}=\bar{\Delta}_z - t_0(n-1)/n$ and according to Eq. (1)

$$\bar{\Delta}_z = (R_1/2)\cdot(\sin\alpha_1\tan\alpha_1)+(R_2/2)\cdot(\sin\bar{\alpha}_2\tan\bar{\alpha}_2)\ . \tag{11}$$

The second term $d\Delta_z/d\lambda\big|_{\lambda=\bar{\lambda}}$ in Eq. (9) is derived as

$$\begin{aligned}\left(d\Delta_z/d\lambda\right)\Big|_{\lambda=\bar{\lambda}} &= \left(d\Delta_z/d\alpha_2\right)\Big|_{\alpha_2=\bar{\alpha}_2}\cdot\left(d\alpha_2/d\theta\right)\Big|_{\theta=\bar{\theta}}\cdot\left(d\theta/d\lambda\right)_{\lambda=\bar{\lambda}}\\ &= \left[(R_2/2)\cdot\sin\bar{\alpha}_2\cdot\left(1+\sec^2\bar{\alpha}_2\right)\right]\cdot\left[1-\left(\bar{L}_{GF}/R_2\cos\bar{\alpha}_2\right)\right]\cdot\left[1/d\cos\bar{\theta}\right],\end{aligned} \tag{12}$$

where the first bracket on the right side of Eq. (12) is obtained from Eq. (1), the second bracket is derived from geometry [14], and the third bracket is the angular dispersion of the grating with $\bar{\theta}$ being the diffraction angle at the central wavelength $\bar{\lambda}$, d is the groove spacing of the grating. The last term in Eq. (9) is the reciprocal of the linear dispersion of the grating with the second mirror R_2 at the central wavelength, which is given as

$$\left(d\lambda/dH\right)\Big|_{H=0} = 2d\cos\bar{\theta}/R_2\ . \tag{13}$$

The tilt angle δ of the cylindrical lens with respect to the plane perpendicular to the optical axis as designated in Fig. 2 can be calculated as

$$\delta = \xi - \left[\tan^{-1}\left(\left(df_s/dH\right)\Big|_{f_s=\bar{f}_s}\right)+\bar{\alpha}_2\right], \tag{14}$$

where $\left(df_s/dH\right)\Big|_{f_s=\bar{f}_s} = \left(df_s/d\alpha_2\right)\Big|_{\alpha_2=\bar{\alpha}_2}\cdot\left(d\alpha_2/d\theta\right)\Big|_{\theta=\bar{\theta}}\cdot\left(d\theta/d\lambda\right)\Big|_{\lambda=\bar{\lambda}}\cdot\left(d\lambda/dH\right)\Big|_{H=0}$, given by $\left(df_s/d\alpha_2\right)\Big|_{\alpha_2=\bar{\alpha}_2} = \left(R\sin\bar{\alpha}_2/2\cos^2\bar{\alpha}_2\right)$, while the other three terms are given in Eqs. (12) and (13).

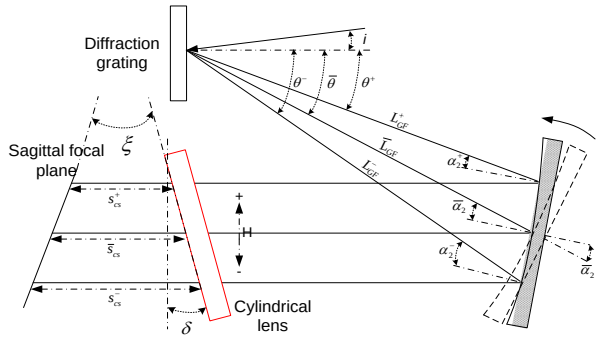

Fig. 2. Broadband astigmatism correction by a tilted cylindrical lens in the tangential view of chief ray-tracing for the different wavelengths in the part of the spectrometer, *i* is the incident angle to the grating.

3. Design procedure for broadband astigmatism-corrected Czerny-Turner spectrometer

A wide bandwidth spanning 600 nm to 1000 nm that is a region of interest in FD-OCT and ultra short pulse measurement was considered. The light was delivered to the entrance of the spectrometer using a single mode fiber. A pinhole can also be used in free space applications. A photonic crystal fiber (PCF) was selected. The numerical aperture (NA, half width at $1/e^2$)

#132486 - $15.00 USD Received 29 Jul 2010; revised 3 Oct 2010; accepted 4 Oct 2010; published 21 Oct 2010

of the fiber depends on wavelength as 0.032 at 600 nm, 0.037 at 700 nm, 0.042 at 800 nm, 0.047 at 900 nm, and 0.052 at 1000 nm. The goal for spectral resolution (SR) was set to 0.1 nm, as the application of FD-OCT that guided this design corresponded to ~1 mm imaging depth in skin (refractive index of skin: ~1.4). The basic parameters of the detector were then set. The number of pixel was chosen to be 8000, which was the next available off-shelf number and more than the minimum number of pixels, 4000, calculated from the bandwidth $\Delta\lambda$ (i.e. 400 nm) and the spectral resolution 0.1 nm (i.e. 400 nm / 0.1 nm). The length of the detector was 80 mm with a pixel size of 10 μm. The diverging beams with different numerical apertures from the PCF were collimated by the first spherical mirror to a reflective diffraction grating. The *F/#* of the first spherical mirror was determined with the NA of the incident light. The *F/#* was calculated to be 11.9 at the central wavelength. The focal length f_1 of the first spherical mirror was chosen as an off-shelf 200 mm. The collimated beam size Φ is calculated to be 16.8 mm by $\Phi = f_1 / (F/\#)$. The NA at the image plane (NA_i) was calculated from the pixel size of the detector using diffraction-limit theory to yield 0.05 at 800 nm. The focal length f_2 of the second mirror was estimated at 175 mm using the beam size Φ and NA_i. f_2 was chosen to be an off-shelf 150 mm, near the estimated value. The collimated beam from the first spherical mirror was dispersed spectrally on the grating surface. The angular spread $\Delta\theta$ was derived using the grating equation, which is given by

$$\Delta\theta = \left(\mathrm{d}\theta / \mathrm{d}\lambda\right)\Big|_{\lambda=\bar{\lambda}} \cdot \Delta\lambda = \left(\Delta\lambda / d \cdot \cos\bar{\theta}\right) . \quad (15)$$

The groove spacing d was calculated using the relation of detector length L, the focal length f_2 and the angular spread $\Delta\theta$ of the full bandwidth 400 nm.

$$d = \left(\Delta\lambda / \cos\bar{\theta}\right) \cdot \left(f_2 / L\right) , \quad (16)$$

where $\bar{\theta}$ was set to 45° to secure sufficient free spectral range as shown in Fig. 3. d was calculated to be 1.1 μm. We selected an off-shelf value of 1.2 μm, which corresponded to 833 lines/mm. The resolving power of the grating was checked to satisfy the condition $(\Phi/d) \geq (\lambda_0/\mathrm{SR})$ [15]. If it was not, Φ would be increased by adjusting the focal length of the first mirror. The tilt of the first mirror, α_1, was selected to be near the smallest angle to avoid obscuration of the rays by the secondary mirror. We chose 12°. The sagittal focal length of the cylindrical lens was chosen to secure some margin between the detector and the cylindrical lens. We chose an off-shelf cylindrical lens with f_{cs} equal 100 mm, n equal 1.5, and t equal 5.2 mm. We optimized the system parameters using the ray-tracing software CODE V to get the best balance of coma. The initial and final parameters are shown in Table. 1. The fixed parameters are shown in Table 2. These values correspond to off-shelf components.

Table 1. Initial and optimized parameters

Variable Parameters	α_1 (°)†	$\bar{\alpha}_2$ (°)	α (°)†	$\bar{\theta}$ (°)	$\bar{L}_{GF}$ (mm)	$\bar{L}_c$ (mm)	δ (°)	L (mm)
Initial	12	0	0	45	150	100	0	80
Final	12	17.3	0	41.8	129.3	102.5	9.1	68.2
† Selected to avoid interference between optics and rays.								

Table 2. Fixed parameters

Fixed parameters	R_1 (mm)	R_2 (mm)	d (μm)	f_{cs} (mm)	t_0 (mm)
Values	400	300	1.2	100	5.2

Before optimization with the cylinder lens, the astigmatism Δ_z at 800nm was calculated to be 21.5 mm using Eq. (1), where α_1 and $\bar{\alpha}_2$ are given in Table 1. The position L_c of the cylindrical lens was calculated to be 100.7 mm using Eq. (6) and (7), which is in close

#132486 - $15.00 USD Received 29 Jul 2010; revised 3 Oct 2010; accepted 4 Oct 2010; published 21 Oct 2010

agreement with the optimized value 102.5 mm. The tilt angle δ of the cylindrical lens was calculated to be 6.4° from Eq. (9) and (14), which is close to the optimized value 9.1°. The optimized layout is shown in Fig. 3(a).

4. Analysis

The spectrometer performance was evaluated to predict the spectral resolution along the length of the detector and power collection. The spectral resolution is defined as the spectral bandwidth that one pixel subtends. The wavelength distribution detected by one pixel can be derived by the convolution of the pixel and the line spread function (LSF) for each pixel. The pixel represents a rectangular function with 10 μm width and the LSF was computed from the ray tracing software. The pixel function and the LSF are shown as a red dotted line and blue solid line in Fig. 3(b), respectively. The convolution was done with respect to the distance along the pixels and then the corresponding convolution with respect to the wavelength was obtained considering the dispersion of the grating. The result is shown in Fig. 3(c). The spectral resolution was measured using two metrics; the full width at half maximum and second, the 80% dip in the separation of the two convolutions as shown in Fig. 3(c) and 3(d).

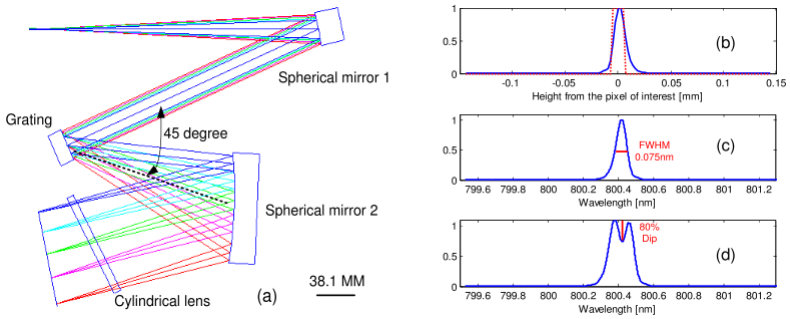

Fig. 3. (a) Optimized layout of the broadband astigmatism-corrected Czerny-Turner spectrometer (b) The pixel function in a red dotted line and the LSF in a blue solid line (c) the convolution over the pixel (d) the 80% dip in the separation of the two convolutions.

To see how much the performance is improved, we compared the new design with recent attempts at astigmatism management and reduction; specifically with a divergent illumination method [14] and a toroidal mirror method [7], respectively, in the same NA condition and using the detector size (i.e. NA_i = 0.05, L = 80 mm, pixel size 10 μm) and grating dispersion. This comparison is more relevant than a comparison with the original implementation as it puts the corrections in the context of other technically viable options for improvement. As seen in Fig. 4, the new method is the only one that meets the requirement for the application at hand of 0.1 nm spectral resolution and more than 50% throughput over the bandwidth. The computed spectral resolutions are shown in Fig. 4(a). For the new design method, the spectral resolution ranges from 0.07 to 0.09 nm for the FWHM and 0.08 to 0.1 nm for the 80% dip over the full bandwidth as shown in Fig. 4(a). Results demonstrate an improvement of at least three times compared to the other solutions. The power percentages collected by the pixel array with 10 μm width were measured and the results are shown in Fig. 4(b). The throughput collected over the full bandwidth is more than 50% as compared to the other solutions that yield collecting powers of less than 20% over most of the spectrum.

#132486 - $15.00 USD Received 29 Jul 2010; revised 3 Oct 2010; accepted 4 Oct 2010; published 21 Oct 2010

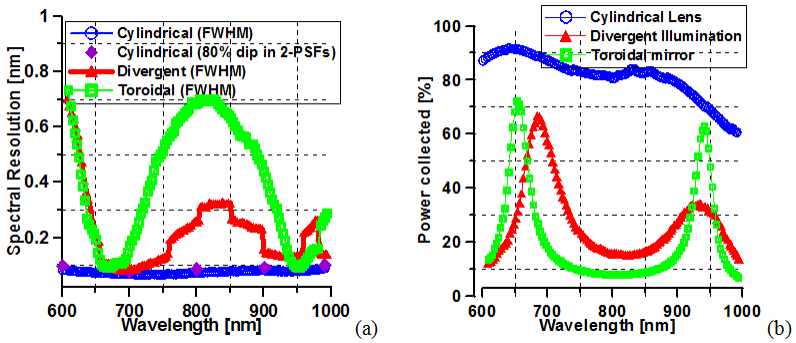

Fig. 4. (a) spectral resolutions over the full bandwidth and (b) power efficiencies collected by the pixel array with 10 μm width for three different methods, the new method reported here (blue), a method based on a divergent wavefront [14] (red), and a method that replaces the spherical mirrors of a traditional Czerny-Turner with toroidal mirrors [7] (green).

5. Conclusion

We have designed a Czerny-Turner type spectrometer using an off-the-shelf cylindrical lens to provide a broadband astigmatism-corrected spectrometer with tilted spherical mirrors. The traditional Czerny-Turner spectrometer, while configured to cancel coma, suffers from astigmatism due to off-axis use of the spherical mirrors. There have been a number of attempts to overcome this limitation including the use of toroidal mirrors. This design enables low cost, practical construction using off-the-shelf optics rather than a custom toroidal mirror or cylindrical grating. This solution is effective over a broad range of parameters according to the specification of the spectrometer designed and does not require restrictions in 1st order parameter selection for astigmatism compensation.

Acknowledgments

This research was funded by the NYSTAR Foundation. We thank Optical Research Associate for providing an educational license for CODE V®.

#132486 - $15.00 USD Received 29 Jul 2010; revised 3 Oct 2010; accepted 4 Oct 2010; published 21 Oct 2010